s-process branching at ^{185}W revised

P. Mohr,[1,2,*] T. Shizuma,[3] H. Ueda,[4] S. Goko,[4] A. Makinaga,[4] K.Y. Hara,[4] T. Hayakawa,[3,5] Y.-W. Lui,[6] H. Ohgaki,[7] and H. Utsunomiya[4]

[1] *Institut für Kernphysik, Technische Universität Darmstadt, Schlossgartenstraße 9, D-64289 Darmstadt, Germany*

[2] *Strahlentherapie, Diakoniekrankenhaus Schwäbisch Hall, D–74523 Schwäbisch Hall, Germany*

[3] *Advanced Photon Research Center, Japan Atomic Energy Research Institute, Tokai, Ibaraki 319-1195, Japan*

[4] *Department of Physics, Konan University, 8-9-1 Okamoto, Higashinada, Kobe 658-8501, Japan*

[5] *National Astronomical Observatory, Osawa 2-21-1, Mitaka, Tokyo 181-8588, Japan*

[6] *Cyclotron Institute, Texas A & M University, College Station, Texas 77843, USA*

[7] *Institute of Advanced Energy, Kyoto University, Gokanosho, Uji, Kyoto 611-0011, Japan*

(Dated: July 18, 2018)

Abstract

The neutron capture cross section of the unstable s-process branching nucleus ^{185}W has been derived from experimental data of the inverse ^{186}W(γ,n)^{185}W photodisintegration taken with monochromatic photon beams from laser Compton scattering. The result of $\sigma = 553 \pm 60\,\mathrm{mb}$ at $kT = 30\,\mathrm{keV}$ leads to a relatively high effective neutron density in the classical s-process of $N_\mathrm{n} = 4.7 \times 10^8\,\mathrm{cm}^{-3}$. A realistic model for the s-process in thermally pulsing AGB stars overestimates the abundance of ^{186}Os significantly because of the relatively small neutron capture cross section of ^{185}W.

PACS numbers: 25.20.-x,25.40.Lw,26.20.+f

*Electronic address: WidmaierMohr@compuserve.de

About half of the nuclei heavier than iron have been synthesized by a series of neutron capture reactions and subsequent β-decays in the so-called astrophysical s-process. This process is called slow because the neutron capture rate is smaller than the β-decay rate for most unstable nuclei. However, there is a number of relatively long-living unstable nuclei with typical half-lives of at least several weeks where neutron capture can compete with the β-decay. Such nuclei are called branching points of the s-process because nucleosynthesis proceeds partly on a neutron-rich branch and partly on a neutron-deficient branch. The analysis of branching ratios allows to determine the effective neutron density $N_{\rm n}$ during the s-process in a simple model, the so-called classical s-process [1]. Alternatively, branching points provide a stringent test for realistic s-process models which describe the dynamics of thermally pulsing asymptotic giant branch (AGB) stars in combination with the corresponding neutron production and nucleosynthesis by neutron-induced reactions [2, 3, 4].

Despite the experimental progress with high-intensity neutron sources and tiny amounts of target material, it still remains extremely difficult to measure the neutron capture cross section of relatively short-living nuclei like ^{185}W with half-lives of $t_{1/2} \ll 1\,$y. This neutron capture cross section for ^{185}W ($t_{1/2} = 75.1\,$d) may be derived from the inverse ^{186}W(γ,n)^{185}W photodisintegration with help of theoretical models.

A first experiment at low energies was performed by Sonnabend *et al.* [5] using bremsstrahlung photons and the photoactivation method. Because of the broad bremsstrahlung spectrum it was not possible to measure the energy dependence of the (γ,n) reaction in that experiment. Additionally, the result had significant systematic uncertainties of about 15 % because of the uncertainties of the shape of the bremsstrahlung spectrum close to its endpoint energy. Therefore we remeasured the (γ,n) cross section of ^{186}W using a tunable monochromatic photon source from laser Compton scattering (so-called Laser Compton Scattering photons, LCS).

The experiment was performed at AIST (Tsukuba, Japan). Photons from a frequency-doubled Nd:YLF Q-switch laser at a wavelength of $\lambda = 526$ nm were 180° scattered from a relativistic electron beam in the storage ring TERAS. The electron energy was varied from 460 to 588 MeV which allowed to produce photons with maximum energies from 7.4 to 12.2 MeV. The initial electron current of about 200 mA in the storage ring combined with the high laser power of 40 W leads to a typical photon intensity of about 10^4/s after collimated into a 2 mm (in diameter) spot at target position which is located roughly 8 m

from the interaction area of the laser photons and electrons. The number of LCS photons decreases during the experiment with the decreasing electron beam current; therefore the electron storage ring was refilled twice a day. Further details on the LCS photon setup at AIST and its application to photonuclear astrophysics can be found in [6, 7, 8, 9].

The target consisted of 1246 mg metallic tungsten powder highly enriched in ^{186}W to 99.79 %. The powder was pressed to a small self-supporting tablet with a diameter of 8 mm. The tablet was mounted into a thin holder made of pure aluminum which does not emit neutrons below its high neutron separation energy of $S_{\rm n} = 13.1$ MeV. The neutrons from the ^{186}W(γ,n)^{185}W photodisintegration were detected using an improved neutron detector that consists of 16 individual ^{3}He counters embedded in two rings in a polyethylene moderator. The so-called ring ratio between the count rates of the inner and outer rings depends on the neutron energy, and hence the ring ratio can be used to estimate the neutron energy. In this experiment the ring ratio varied between 2.5 and 4.4 leading to average neutron energies of about 1.2 MeV at highest photon energies and of about 0.3 MeV at lower neutron energies for the measurements close above the threshold. Further experimental details are given in [9]. The efficiency of the neutron detector is given in Fig. 2 of [10]; the efficiency was measured at the average neutron energy 2.14 MeV using a calibrated ^{252}Cf source and the energy dependence was determined by a MCNP simulation.

The number of neutrons $n_{\rm exp}$ emitted in the photodisintegration experiment is directly related to the (γ,n) cross section $\sigma(E_\gamma)$ for ideally monochromatic photons with energy E_γ

$$n_{\rm exp} = N_\gamma \times N_{\rm T} \times h \times \sigma(E_\gamma), \tag{1}$$

where N_γ is the number of photons, h is the correction factor for a thick-target measurement, $h = (1-e^{-\mu t})/\mu t$ with the target thickness t and the attenuation coefficient of target material μ, and $N_{\rm T}$ is the number of target atoms per area. For the realistic photon spectrum with a low-energy tail the product $N_\gamma \times \sigma(E_\gamma)$ in Eq. (1) has to be replaced by the integral

$$N_\gamma \times \sigma(E_\gamma) \;\rightarrow\; \int n_\gamma(E_\gamma) \times \sigma(E_\gamma)\, dE \tag{2}$$

with the photon energy distribution $n_\gamma(E_\gamma)$. In Eq. (2), let us rewrite $\sigma(E_\gamma)$ in the Taylor series,

$$\sigma(E_\gamma) = \sigma(E_0) + \sigma^{(1)}(E_0)(E_\gamma - E_0) + \frac{1}{2}\sigma^{(2)}(E_0)(E_\gamma - E_0)^2 + \frac{1}{6}\sigma^{(3)}(E_0)(E_\gamma - E_0)^3 + \cdots, \tag{3}$$

where $\sigma^{(i)} = d^i\sigma(E)/dE^i$. When the average energy is chosen for E_0, putting the Taylor series into Eq. (2) ends up with

$$\int n_\gamma(E_\gamma) \times \sigma(E_\gamma)\, dE_\gamma = N_\gamma\{\sigma(E_0) + s_2(E_0) + s_3(E_0) + \cdots\}, \tag{4}$$

where $s_2(E_0) = \frac{1}{2}\sigma^{(2)}(E_0)\,[\bar{E}_\gamma^2 - E_0^2]$ and $s_3(W_0) = \frac{1}{6}\sigma^{(3)}(E_0)[\bar{E}_\gamma^3 - 3E_0\bar{E}_\gamma^2 + 2E_0^3]$ with $\bar{E}_\gamma^i = \int n_\gamma(E_\gamma)E_\gamma^i dE_\gamma/N_\gamma$. Note that the first derivative term $\sigma^{(1)}$ explicitly vanishes.

Experimentally, the whole Taylor series in the parenthesis in Eq. (4) is obtained by using the numbers of neutrons, target nuclei per unit area, and incident γ rays. In contrast, the first term $\sigma(E_0)$, which is the cross section at the average γ energy, is obtained provided that the s_2 and the s_3 *etc.* are subtracted.

We evaluated the higher-order terms which include $\sigma^i(E_0)$ and $\bar{E}_\gamma^i$, where the energy dependence of the cross section was derived by the best fit to the experimental quantity corresponding to the whole Taylor series plotted at the average γ energy. Details of the evaluation will be given in a separate paper, including a more general discussion on the methodology of deducing cross sections in a quasi-monochromatic γ-induced reaction. The subtraction of the higher-order terms resulted in a few % increase in $\sigma(E_0)$ in the energy region of astrophysical relevance below 8.6 MeV and a decrease of 12 - 20 % above 9 MeV.

A typical photon spectrum $n_\gamma(E_\gamma)$ is shown by the dashed line in Fig. 1. The time variation of the photon spectrum which is sensitive to the electron beam size at the collision point was carefully investigated. The analysis of the photon spectrum measured with the HPGe detector showed that the variation of the electron beam current during individual measurements did not result in a significant change in the beam size. Thus, both the average γ energy and the fraction of the photon spectrum above the neutron threshold were determined with sufficient accuracy.

The number of incoming photons was monitored during the experiment using a large-volume 8 x 12 inches (diameter x length) NaI(Tl) summing crystal. The pulse height in the sum spectrum is proportional to the number of LCS photons which have the 2 kHz repetition rate of the laser. A typical spectrum of the NaI(Tl) summing crystal is shown in Fig. 2.

The measured photodisintegration cross section from the threshold of ^{186}W at S_n = 7194 keV up to about 11 MeV is shown in Fig. 3. The systematic uncertainties are dominated by the efficiency of the neutron detector (5 %) and the γ-ray flux (3 %). At energies close to the threshold statistical uncertainties are comparable to the above systematic uncertainties;

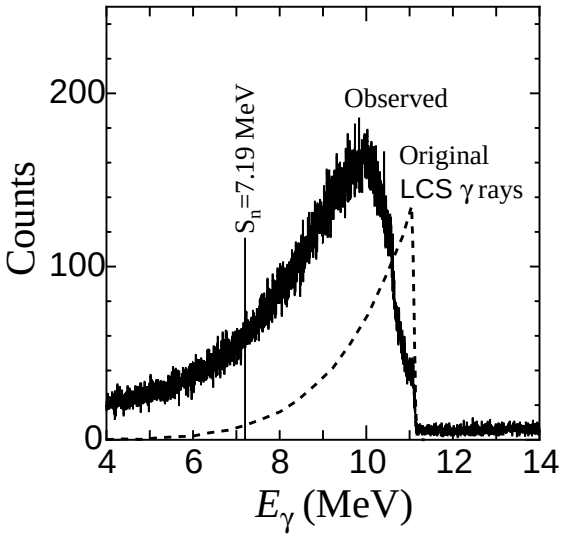

FIG. 1: Photon spectrum measured with a 120 % relative efficiency germanium (HPGe) detector (full line) along an incident photon spectrum (dashed line). For the analysis of the measured HPGe spectrum to obtain the incident LCS photon energy spectrum, see [9]. The neutron separation energy $S_{\rm n}$ of ^{186}W is indicated by a vertical line.

at higher energies statistical uncertainties are small. The error bars shown in Fig. 3 include both systematic and statistical uncertainties. Compared to the previous experiment [5], the uncertainties have been reduced significantly. More importantly, the energy dependence of the photodisintegration cross section has been determined down to the threshold. Earlier data at higher energies [11, 12, 13] are in reasonable agreement with our new data but have larger uncertainties especially at lower energies.

There is no direct way to derive the neutron capture cross section of the s-process branching nucleus ^{185}W from the photodisintegration cross section of the ^{186}W$(\gamma,{\rm n})^{185}$W reaction. Following [5], the theoretical prediction is adjusted to the experimental data using a normalization factor $f_{(\gamma,{\rm n})}$. The same normalization factor $f_{({\rm n},\gamma)} = f_{(\gamma,{\rm n})}$ is used to scale the theoretical prediction of the neutron capture cross section. This procedure, its reliability and limitations are discussed in detail in [5]. Here we repeat briefly the basic idea. For the above reactions the main ingredients for the statistical model predictions are the photon strength function, the neutron-nucleus optical potential, and the level densities. It has turned out that the most sensitive ingredient is the electric dipole (E1) photon strength function which is usually extrapolated from the GDR to lower energies. Both $\sigma(\gamma,{\rm n})$ and $\sigma({\rm n},\gamma)$ are pro-

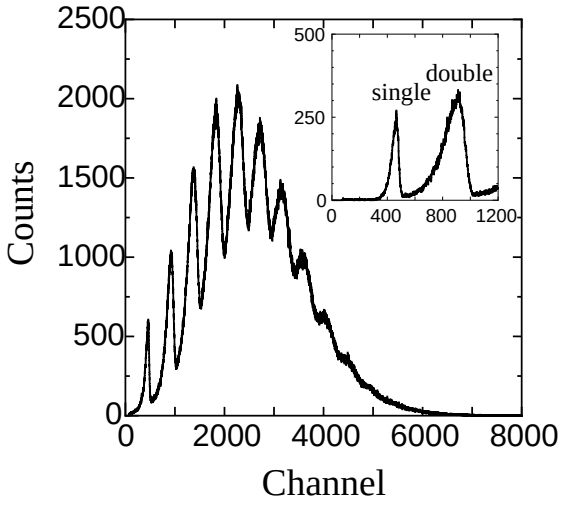

FIG. 2: Photon spectrum measured with a 8 x 12 inches NaI(Tl) detector. The number of photons per laser pulse can be extracted from the average pulse output of the summing crystal. In the shown spectrum the average photon number per laser pulse is 6.2 leading to a photon intensity of 1.2×10^4/s. The inset shows a similar spectrum measured with reduced laser power; here one finds mainly one or two LCS photons per laser pulse.

portional to this strength function, and consequently the above assumption $f_{(\mathrm{n},\gamma)} = f_{(\gamma,\mathrm{n})}$ is justified if all other ingredients of the model are precisely known. The assumption approximately remains valid for realistic cases to within $10\,\% - 20\,\%$ because of the uncertainties of the other ingredients. An obvious additional requirement to the theoretical model is the correct prediction of the energy dependence of the photodisintegration cross section which is fulfilled for both calculations of [5], at least at energies close above the threshold (see Fig. 3).

Two statistical model (or Hauser-Feshbach, HF) calculations with different ingredients (called I and II) were used in [5] to derive the neutron capture cross section from the experimental photodisintegration data. Model I predicts a neutron capture cross section of $\sigma_{\mathrm{pre}} = 600\,\mathrm{mb}$ at $kT = 30\,\mathrm{keV}$. Together with the scaling factor $f_{(\gamma,\mathrm{n}),I} = 1.0$ and the above assumption of $f_{(\mathrm{n},\gamma)} = f_{(\gamma,\mathrm{n})}$ one obtains the experimentally corrected cross section of $\sigma_{\mathrm{exp}} = 600\,\mathrm{mb}$. This value is already Maxwellian averaged for a temperature $kT = 30\,\mathrm{keV}$, and it includes a minor correction for thermally excited states in ^{185}W at such temperatures. The corresponding values for model II are $\sigma_{\mathrm{pre}} = 657\,\mathrm{mb}$, $f_{(\gamma,\mathrm{n}),II} = 0.77$, and $\sigma_{\mathrm{exp}} = 506\,\mathrm{mb}$. Averaging both values of σ_{exp}, the final result for the neutron capture cross section of ^{185}W is

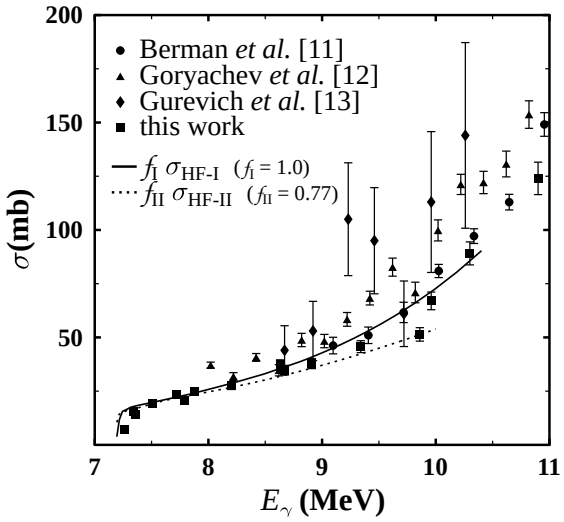

FIG. 3: Photodisintegration cross section of the reaction ^{186}W(γ,n)^{185}W. The new data are shown as squares. Previous data of [11, 12, 13], shown as circles, triangles, and diamonds, do not cover the astrophysically relevant energy region close above the threshold at $S_{\rm n} = 7194\,$keV. The statistical model predictions (as taken from Ref. [5]) have been scaled by factors of $f_I = 1.0$ (full line) and $f_{II} = 0.77$ (dotted line) to fit the new experimental data (see text).

$\sigma = 553 \pm 60\,$mb. The uncertainty of this value is dominated by theoretical uncertainties for the relation between the (γ,n) and (n,γ) reactions which can be estimated to be 47 mb from the deviations of the two calculated values. The experimental uncertainties of the present (γ,n) data are much smaller.

The new result is about 20 % lower than the previous result of [5]; taking into account the 15 % uncertainty of the experimental data of [5], there is reasonable agreement between the previous data and the new experimental results. The new result is also slightly lower than the adopted value ($\sigma_{\rm adopt} = 703 \pm 113\,$mb) of a recent compilation [14]; the value from the compilation is based on several theoretical predictions [15, 16, 17].

There are interesting astrophysical consequences of this new result for the neutron capture cross section of ^{185}W. The derived neutron density $N_{\rm n}$ in the classical s-process scales inversely with the neutron capture cross section of the analyzed branching nucleus. A relatively high value of $N_{\rm n} = (4.7^{+1.4}_{-1.1}) \times 10^8\,{\rm cm}^{-3}$ is obtained from the new value of $\sigma = 553\,$mb. A realistic s-process model [2, 3, 4] describes the s-process during thermally pulsing AGB stars. A cross section of about 1000 mb is required to reproduce the abundance of ^{186}Os which depends on the branching at ^{185}W. The previous value of $\sigma = 687\,$mb [5] leads to an

overproduction of ^{186}Os of 20 %; taking into account the uncertainties of the solar osmium abundance and of the ^{186}Os neutron capture cross section (as discussed in [5]), the *s*-process model prediction corresponds to an error at the $3\,\sigma$ level. The even smaller cross section of $\sigma = 553\,\mathrm{mb}$ of this work sharpens the discrepancy with the otherwise successful model of the *s*-process. Hence the new data provide further restrictions for realistic *s*-process models and may contribute to improve such models.

Acknowledgments

We thank N. Pietralla for the borrowing of the enriched target. Discussions with H. Beer, R. Gallino, F. Käppeler, A. Mengoni, T. Rauscher, and A. Zilges are gratefully acknowledged. This work was supported in part by the Japan Private School Promotion Foundation and by the Japan Society for the Promotion of Science.

---

[1] R. A. Ward, M. J. Newman, and D. D. Clayton, Astrophys. J. Suppl. **31**, 33 (1976).

[2] R. Gallino, C. Arlandini, M. Busso, M. Lugaro, C. Travaglio, O. Straniero, A. Chieffi, and M. Limongi, Astrophys. J. **497**, 388 (1998).

[3] C. Arlandini, F. Käppeler, K. Wisshak, R. Gallino, M. Lugaro, M. Busso, M., and O. Straniero, O., Astrophys. J. **525**, 886 (1999).

[4] M. Busso, R. Gallino, D. L. Lambert, C. Travaglio, and V. V. Smith, Astrophys. J. **557**, 802 (2001).

[5] K. Sonnabend, P. Mohr, K. Vogt, A. Zilges, A. Mengoni, T. Rauscher, H. Beer, F. Käppeler, and R. Gallino, Astrophys. J. **583**, 506 (2003).

[6] H. Ohgaki *et al.*, IEEE Trans. Nucl. Sci. **38**, 386 (1991).

[7] H. Toyokawa *et al.*, IEEE Trans. Nucl. Sci. **47**, 1954 (2000).

[8] H. Utsunomiya, Y. Yonezawa, H. Akimune, T. Yamagata, M. Ohta, M. Fujishiro, H. Toyokawa, and H.Ohgaki, Phys. Rev. C **63**, 018801 (2001).

[9] H. Utsunomiya, H. Akimune, S. Goko, M. Ohta, H. Ueda, T. Yamagata, K. Yamasaki, H. Ohgaki, H. Toyokawa, Y.-W. Lui, T. Hayakawa, T. Shizuma, E. Khan, and S. Goriely, Phys. Rev. C **67**, 015807 (2003).

[10] K.Y. Hara, H. Utsunomiya, S. Goko, H. Akimune, T. Yamagata, M. Ohta, H. Toyokawa, K. Kudo, A. Uritani, Y. Shibata, Y.-W. Lui, and H. Ohgaki, Phys. Rev. D **68**, 072001 (2003).

[11] B. L. Berman, M. A. Kelly, R. L. Bramblett, J. T. Caldwell, H. S. Davis, and S. C. Fultz, Phys. Rev. **185**, 1576 (1969).

[12] A. M. Goryachev and G. N. Zalesnyĭ, IZV. An. KazSSR **6**, 8 (1978).

[13] G. M. Gurevich, L. E. Lazareva, V. M. Mazur, S. Yu. Merkulov, G. V. Solodukhov, and V. A. Tyutin, Nucl. Phys. **A351**, 257 (1981).

[14] Z. Y. Bao, H. Beer, F. Käppeler, F. Voss, and K. Wisshak, At. Data Nucl. Data Tables **76**, 70 (2000).

[15] T. Rauscher and F.-K. Thielemann, At. Data Nucl. Data Tables **75**, 1 (2000).

[16] J. Holmes, S. Woosley, W. Fowler, and B. Zimmerman, At. Data Nucl. Data Tables **18**, 305 (1976).

[17] F. Käppeler, S. Jaag, Z. Y. Bao, and G. Reffo, Astrophys. J. **366**, 605 (1991).